Hindawi Publishing Corporation
Research Letters in Physical Chemistry
Volume 2007, Article ID 96251, 5 pages
doi:10.1155/2007/96251

Research Letter

Fourier-Domain Analysis of Hydriding Kinetics Using Pneumato-Chemical Impedance Spectroscopy

P. Millet,[1] C. Decaux,[2] R. Ngameni,[1] and M. Guymont[1]

[1] *Institut de Chimie Moléculaire et des Matériaux, CNRS UMR 8182, Université Paris-Sud 11, 15 rue Georges Clémenceau, 91405 Orsay Cedex, France*
[2] *Compagnie Européenne des Technologies de l'Hydrogène (CETH), Innov' Valley Entreprise, Route de Nozay, 91461 Marcoussis Cedex, France*

Correspondence should be addressed to P. Millet, pierre.millet@u-psud.fr

Received 10 July 2007; Accepted 12 September 2007

Recommended by Claudio Fontanesi

Analysis of phase transformation processes observed in hydrogen absorbing materials (pure metals, alloys, or compounds) is still a matter of active research. Using pneumato-chemical impedance spectroscopy (PIS), it is now possible to analyze the mechanism of hydriding reactions induced by the gas phase. Experimental impedance diagrams, measured on activated $LaNi_5$ in single- and two-phase domains, are reported in this paper. It is shown that their shape is mostly affected by the slope of the isotherm at the measurement point. By considering the details of the multistep reaction paths involved in the hydriding reaction, model impedance equations have been derived for single- and two-phase domains, and fitted to experimental impedance diagrams. The possibility of separately measuring surface and phase transformation resistances, hydrogen diffusion coefficient, and hydrogen solubility in each composition domain is discussed.

1. INTRODUCTION

Analysis of phase transformation processes induced by hydrogen in metals is still a matter of active research. The challenges of identifying the growth mode of hydride phases and measuring the microscopic rate parameters associated with their formation are complicated by the presence of a strong and irreducible hysteresis. In the literature, the hydriding kinetics of palladium and intermetallic powdered electrodes have been more specifically investigated [1–3], in both single-phase domains (SPDs) and two-phase domains (TPDs). Many authors have used electrochemical harmonic perturbations, arguing that in spite of hysteresis, these systems were linear [3, 4], although they are obviously not. Surprisingly, they observed that impedance diagrams measured in TPDs, where hysteresis is large, were similar in shape to those measured in SPDs where there is no hysteresis, although different chemical processes are taking place. Probably because of this similitude, experimental impedance diagrams measured in TPDs are commonly and unduly fitted using equations derived for SPDs [3]. It is therefore difficult to determine, from such results, what is the growth mode of hydride phases and what is the rate contribution of the phase transformation process to the overall hydriding kinetics.

Investigating the electrochemical insertion of hydrogen in palladium, Millet [5] observed the existence of reversible thermodynamic paths in TPDs, in the potential domain bracketed by the main absorption and desorption plateau potentials. These results provided a first indication that most experimental data reported in the literature on TPDs were not characteristic of phase transformation processes. More recently, impedance spectroscopy was extended to solid-gas reactions [6]. Using this spectroscopy, Millet et al. were able to measure pneumato-chemical impedance diagrams in TPDs and to show [7] that even along the main pressure plateau, impedance diagrams were similar in shape to those measured in solid solution domains. Therefore, there is still a need to clarify the role of the phase transformation step in the overall hydriding kinetics. In this work, we report on impedance diagrams measured at 298 K on $LaNi_5$, in SPDs and TPDs. Analytical impedance expressions based on microscopic multistep reaction mechanisms are derived for

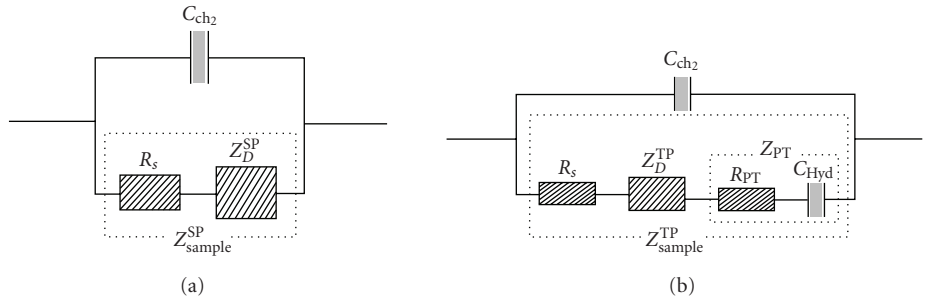

Figure 1: Equivalent electric circuits used to model hydriding reactions: (a) in single-phase domains; (b) in two-phase domains.

each composition domain. It is shown that they both have the same graph, although the physical meaning of microscopic rate parameters is different.

2. EXPERIMENTAL SECTION

The volumetric experimental setup used to measure pneumato-chemical impedances has been described in detail elsewhere [6, 8]. Briefly, a stainless steel reference chamber (Ch_1) is connected to a thermostated reaction chamber (Ch_2) in which 2.9 g of $LaNi_5$(Alfa Aesar GmbH, Karlsruhe, Germany) are placed. The hydriding step Δ(H/M) is controlled by transferring small amounts of hydrogen from Ch_1 to Ch_2. Typically, $0.05 < \Delta(\mathrm{H/M}) < 0.15$. During each gas transfer experiment, transient pressures $P_1(t)$ and $P_2(t)$ are synchronously sampled, providing raw kinetic data. The hydrogen mass flow $dn/dt(t)$ entering the reaction chamber is obtained from the law of ideal gases:

$$\frac{dn}{dt}(t) = \frac{V_1}{RT}\frac{dP_1}{dt}. \tag{1}$$

The basic principles of PIS analysis have been presented elsewhere [6]. Experimental pneumato-chemical impedance diagrams $Z_2^{\exp}(\omega)$ are obtained using the theory of linear and time-invariant systems [9]:

$$Z_2^{\exp}(\omega) = \frac{P_2(\omega)}{dn/dt(\omega)}. \tag{2}$$

ω denotes the pulsation in rad·s^{-1}. $P_2(\omega)$ and $dn/dt(\omega)$ are the Fourier transform of $P_2(t)$ and $dn/dt(t)$. $Z_2(\omega)$ is a pneumato-chemical impedance, by analogy with electrochemical systems.

3. MODELING

Model impedances $Z_2^{\mathrm{mod}}(\omega)$ are obtained as follows. First, Z^{sample} (the impedance of the hydrogen absorbing sample) is obtained by considering the reaction path associated with the hydriding reaction:

(step 1-a) $H_2(g)H_2^{\mathrm{surface}}$,
(step 1-b) $H_2^{\mathrm{surface}}2H_{\mathrm{ad}}^{\mathrm{surface}}$,
(step 1-c) $H_{\mathrm{ad}}^{\mathrm{surface}}H_{\mathrm{ab}}^{\text{sub-surface}}$,
(step 2) $H_{\mathrm{ab}}^{\text{sub-surface}}$ diffusion H_{bulk},
(step 3) H_{bulk} phase transformation hydride.

H_{ad} denotes a surface ad atom, H_{ab} denotes a hydrogen atom absorbed in the metal subsurface and H_{bulk} denotes a hydrogen atom in bulk regions. In SPDs, the reaction sequence ends at step 2. In TPDs, it is necessary to take into account the phase transformation process (step 3). In the followings, the impedance associated with (step 1-a) is not considered because pure hydrogen is used in the experiments. Also, steps 1-b and 1-c are considered as one single step of surface chemisorption. The surface step and the phase transformation step are modeled assuming a linear pressure (concentration)—mass flow relationship (a frequency independent surface resistance R_s and R_{PT}). Analytical expressions of $Z_2^{\mathrm{mod}}(\omega)$ are derived in SPDs and TPDs by considering the electrical analogies of Figure 1 and by applying Kirchhoff's laws of electrical networks. A capacitance C_{Ch2} is added in parallel to Z^{sample} to account for the volume of the reaction chamber where H_2 can accumulate.

3.1. Single-phase domains

The impedance associated with the diffusion step is obtained by solving Fick's laws of diffusion in spherical coordinates [10]:

$$\begin{aligned} Z_D^{\mathrm{SP,sphere}}(\omega) &= \frac{r}{D_H}\frac{\partial P_{H_2}}{\partial C_H}\frac{th(u)}{u - th(u)} \\ &= R_D^{\mathrm{SP,sphere}}\frac{th(u)}{u - th(u)} \\ &= R_D^{\mathrm{SP,sphere}}\frac{1}{u\coth(u) - 1}, \end{aligned} \tag{3}$$

where $u = \sqrt{j\omega r^2/D_H}$. The expression of $R_D^{\mathrm{SP,sphere}}$ is adapted here to solid-gas reactions:

$R_D^{\mathrm{SP,sphere}} = (r/D_H)(\partial P_{H_2}/\partial C_H)$ in Pa/(mole·s^{-1}·cm^{-2}); $\partial P_{H_2}/\partial C_H$ is the slope of the isotherm at the measurement point; r is the mean particle radius in cm and D_H in cm^2·s^{-1} is the hydrogen diffusion coefficient. ω is the pulsation in rad·s^{-1}. The low frequency limit of (3) is

$$Z_D^{\mathrm{SP,sphere}}(\omega) \approx \frac{R_D^{\mathrm{SP,sphere}}}{5} - j\frac{3D_H R_D^{\mathrm{SP,sphere}}}{\omega r^2} = R_{\mathrm{in}} - j\frac{1}{\omega C_{\mathrm{in}}}. \tag{4}$$

In Nyquist coordinates, (4) is the equation of a complex and semi-infinite line of constant real value, parallel to the imaginary axis. R_{in} is the insertion resistance in $Pa \cdot mol^{-1} \cdot s \cdot cm^2$ (real part of the low frequency limit of the diffusion impedance). C_{in} is the insertion capacitance of the sample expressed per unit area of solid-gas interface in $mol \cdot Pa^{-1} \cdot cm^{-2}$.

In SPDs, the total pneumato-chemical impedance $Z_2^{SP,mod}(\omega)$ of the reaction chamber Ch_2 is finally

$$Z_2^{SP,mod}(\omega) = \left(\frac{1}{jC_2\omega + \left(1/\left(R_s + Z_D^{SP,sphere}\right)\right)} \right). \quad (5)$$

3.2. Two-phase domains

In TPDs, the diffusion impedance is different from the one in SPDs because boundary conditions are different and it is necessary to take into account the phase transformation (PT) process. Assuming that the hydriding reaction of $LaNi_5$ proceeds, as for palladium [5], according to a moving boundary mechanism (MBM), hydrogen diffusion takes place in the surface growing hydride layer and the step of hydride precipitation takes places at the α-β interphase interface (step 3). In the gas transfer experiments presented here, the hydriding step Δ(H/M) is small: the position $\xi(t)$ of the α-β interphase plan measured from the surface can be considered as time-invariant and $C_H(\xi)$ is a point of constant concentration. Then, the expression derived by Wang [11] for spherical particles applies and

$$Z_D^{TP,sphere}(\omega) = R_D^{TP,sphere} \frac{th(\varepsilon u)}{u - th(\varepsilon u)}, \quad (6)$$

where $R_D^{TP,sphere} = R_D^{SP,sphere} = (r/D_H)(\partial P_{H_2}/\partial C_H)$ in $Pa/(mole \cdot s^{-1} \cdot cm^{-2})$; $\varepsilon = \lfloor 1 - (1 - X_\beta)^{1/3} \rfloor$; $X_\beta = V_\beta/(V_\alpha + V_\beta)$; V_α and V_β denotes the volume of the α phase and β phase in two-phase domains. The low frequency limit of (6) is on the real axis:

$$Z_D^{TP,sphere}(\omega) \approx R_D^{TP,sphere} \frac{\varepsilon}{1 - \varepsilon}. \quad (7)$$

When ε is close to unity (a situation found in SPDs), $Z_D^{TP,sphere}(\omega)$ is so large that a capacitive behavior is observed at low frequencies. When $0 < \varepsilon < 1$ (a situation found in TPDs), the value $Z_D^{TP,sphere}(\omega)$ is directly related to the value of ε.

Next to $Z_D^{TP,sphere}(\omega)$ is the phase transformation impedance $Z_{PT}(\omega)$, which has a resistance component R_{PT} (to account for the kinetics of the chemical phase transformation taking place at ξ) and a capacitance component C_{hyd} (to account for the increased hydrogen solubility due to the formation of the hydride phase) (Figure 1(b)). Since all these reactions steps are connected in series, it follows that

$$Z_{PT}(\omega) = R_{PT} - j\frac{1}{\omega C_{PT}}, \quad (8)$$

$$Z_{sample}^{TP}(\omega) = R_s + \quad Z_D^{TP,sphere} + R_{PT} - j\,\frac{1}{\omega C_{Hyd}}. \quad (9)$$

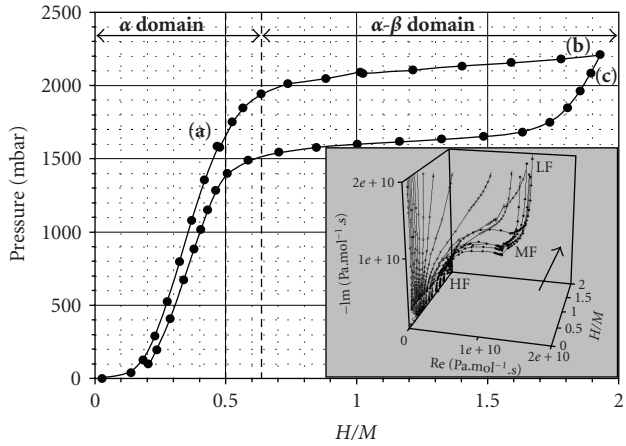

FIGURE 2: Partial isotherm measured on $LaNi_5$ at 298 K. Insert: experimental pneumato-chemical impedances measured during absorption as a function of H/M.

In TPDs, the total pneumato-chemical impedance $Z_2^{TP,mod}(\omega)$ of the reaction chamber Ch_2 is finally

$$Z_2^{TP,mod}(\omega) = \left(\frac{1}{\left(jC_2\omega + \left(1/\left(R_s + Z_D^{TP,sphere} + R_{PT} - j\left(1/C_{Hyd}\omega\right)\right)\right)\right)} \right). \quad (10)$$

When the phase transformation process is fast (this is the case for a fully activated sample), R_{PT} is small. Although $Z_D^{TP,sphere}(\omega)$ is purely real at low frequencies (see (7), the capacitance C_{hyd} connected in series is such that (10) is similar to (5), and both equations have similar graphs although the two models are based on different reaction paths. When the phase transformation process is slow, R_{PT} is high and $Z_D^{TP,sphere}(\omega)$ becomes analogue to $Z_D^{TP,sphere}(\omega)$. Equations (10) and (5) also have the same graph. The value of R_{PT} can be obtained from (9) by substracting R_s (measured in SPDs) to the experimental HF resistance measured in TFDs.

4. RESULTS AND DISCUSSION

A partial pressure-composition isotherm, measured at 298 K on a fully activated $LaNi_5$ sample, is plotted in Figure 2 (the maximum composition at 298 K, not represented here, is H/M $\approx$ 5.8). The powdered bed is made of particles of homogeneous size and the total solid-gas interface is assumed to remain constant (with a mean particle radius $\approx$ 5 μm and 2.9 g of sample, S $\approx$ 2100 cm^2). At low hydrogen content, a single-phase solid solution of hydrogen (α-$LaNi_5$) is formed. As the hydrogen content increases, a substoechiometric hydride phase ($LaNi_5H_{6-x}$ or β-$LaNi_5$ phase) begins to form and a two-phase domain with a pressure plateau develops. Each data point of Figure 2 corresponds to one gas transfer experiment. Impedance diagrams measured as a function of H/M along the absorption branch of the isotherm are plotted in the insert of Figure 2. They are mostly capacitive in shape in SPDs, but a characteristic semicircle appears in TPDs in

Table 1: Microscopic rate parameters obtained by fitting (5) and (10) to the experimental impedances of Figure 3. $r = 5\,\mu$m.

	Curves (a) and (c)		Curve (b)	
	fit (5)	fit (10)	fit (5)	fit (10)
HF resistance ($Pa\cdot mol^{-1}\cdot s$)	$(4.3 \pm 0.2) \times 10^{9}$	$(4.8 \pm 0.2) \times 10^{9}$	$(16.0 \pm 0.8) \times 10^{9}$	$(16.0 \pm 0.8) \times 10^{9}$
D_H ($cm^2\cdot s^{-1}$)	$(5.2 \pm 0.3) \times 10^{-10}$	$(6.3 \pm 0.3) \times 10^{-10}$	$(12.5 \pm 0.6) \times 10^{-10}$	$(6.9 \pm 0.3) \times 10^{-10}$
LF capacitance ($mol\cdot Pa^{-1}$)	$(1.2 \pm 0.1) \times 10^{-8}$	$(1.3 \pm 0.1) \times 10^{-8}$	$(10.9 \pm 0.5) \times 10^{-8}$	$(9.9 \pm 0.5) \times 10^{-8}$

high-frequency (HF) regions, as reported in [7]. It is not possible within the format of this research letter to produce a full account of these results but the kind of information which can be obtained from such impedance diagrams, in SPDs and TPDs, is more specifically analyzed. In particular, the possibility of measuring the rate contribution of the phase transformation process on the overall hydriding kinetics is discussed.

The impedance diagram measured in the TPD just before reversing the absorption scan (point (b), Figure 2) is plotted in Figure 3 (curve (b)) in Nyquist coordinates. The characteristic HF semicircle is the signature of the parallel connection of the capacitance C_{Ch2} (in $mol\cdot Pa^{-1}$) associated with the dead volume of the reaction chamber, and a pneumato-chemical resistance in $Pa\cdot mol^{-1}\cdot s$. This resistance is the sum of R_s and R_{PT} (steps 1-b, 1-c, and 3). When the scan is reversed, the impedance diagram (curve (c) in Figure 3, corresponding to datapoint c in Figure 2) is mostly capacitive in shape, and identical to the one measured symmetrically in the SPD (curve (a) in Figure 3 corresponds to datapoint a in Figure 2). Their frequency contributions are less well-separated than for point (b), for the reasons analyzed elsewhere [8]. Although point (c) is located in the two-phase domain (between the absorption and desorption pressure plateaus), this is also a domain where reversible processes are taking place (only hydrogen transport by diffusion and surface desorption), just like for point (a). Because of hysteresis, the desorption process is not fuelled by the phase transformation (dissolution of the hydride) but by hydrogen reversibly stored in the sample.

Using an automated least-square fitting procedure, the three experimental impedance diagrams of Figure 3 were fitted using model (5) and (10). Results are compiled in Table 1. Concerning HF resistances, values measured from curves (a) and (c) can be fully attributed to the surface resistance R_s. For curve (b), the HF resistance is the sum $R_s + R_{PT}$. Therefore, R_{PT} values in TPDs cannot be directly measured from the experimental impedance diagram but estimated by substracting R_s contributions (measured in SPDs) to the HF resistance. From the data of Table 1, $R_{PT} \approx 1 \times 10^{10}\ Pa\cdot mol^{-1}\cdot s$, larger than R_s by a factor of two. Concerning LF capacitances, values measured for points (a) and (c) are related to the hydrogen solubility and the formation of interstitial solid solutions. In TFDs (point (b)), a larger capacitance associated with the phase transformation processes is measured.

5. CONCLUSIONS

Using pneumato-chemical impedance spectroscopy, experimental impedance diagrams have been measured in single- and two-phase domains during the hydriding reaction of $LaNi_5$. A strong correlation is observed between the shape of the experimental impedance diagrams and the slope of the isotherms at the measurement point. Analytical model impedance equations have been derived to account for the hydriding reaction in single- and two-phase domains. Whereas the two model equations have the same graph, the meaning of the microscopic rate parameters is different, offering the possibility of measuring the rate contribution of the phase transformation process. Values of microscopic rate parameters measured as a function of the hydrogen composition during activation of $LaNi_5$ and along hysteresis loops will be reported in a subsequent communication.

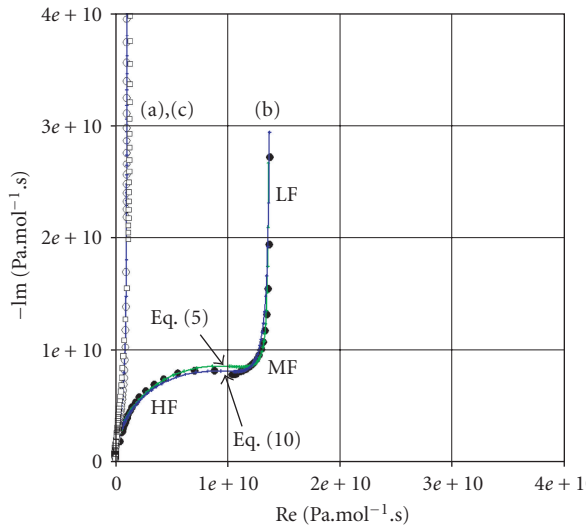

Figure 3: Nyquist plots of the experimental impedances associated with datapoints (a, □), (b,•), and (c, o) in Figure 2. Model impedances (—) using (5) and (10).

ACKNOWLEDGMENT

The financial support from the French Agence Nationale de la Recherche, within the frame of the Plan d'Action National sur l'Hydrogène, EolHy project (ANR-06-PANH—008-06), is acknowledged.

REFERENCES

[1] T.-H. Yang and S.-I. Pyun, "Hydrogen absorption and diffusion into and in palladium: *ac*-impedance analysis under impermeable boundary conditions," *Electrochimica Acta*, vol. 41, no. 6, pp. 843–848, 1996.

[2] T.-H. Yang and S.-I. Pyun, "An investigation of the hydrogen absorption reaction into, and the hydrogen evolution reaction from, a Pd foil electrode," *Journal of Electroanalytical Chemistry*, vol. 414, no. 2, pp. 127–133, 1996.

[3] L. O. Valøen and R. Tunold, "The electrochemical impedance of metal hydride electrodes," *Journal of Alloys and Compounds*, vol. 330–332, pp. 810–815, 2002.

[4] W. Zhang, M. P. S. Kumar, S. Srinivasan, and H. J. Ploehn, "*Ac*-impedance studies on metal hydride electrodes," *Journal of the Electrochemical Society*, vol. 142, no. 9, pp. 2935–2943, 1995.

[5] P. Millet, "Thermodynamic paths in the two-phases domain of the PdH system and a method for kinetic analysis," *Electrochemistry Communications*, vol. 7, no. 1, pp. 40–44, 2005.

[6] P. Millet, "Pneumatochemical impedance spectroscopy. 1. Principles," *Journal of Physical Chemistry B*, vol. 109, no. 50, pp. 24016–24024, 2005.

[7] P. Millet and S. A. Grigoriev, "Pneumato-chemical impedance spectroscopy for analyzing hydogen sorption and desorption reactions in metal hydride systems," *International Scientific Journal for Alternative Energy and Ecology*, vol. 47, no. 3, pp. 22–28, 2007.

[8] P. Millet, C. Decaux, R. Ngameni, and M. Guymont, submitted to *Review of Scientific Instruments*.

[9] A. Ichikawa and H. Katayama, *Linear Time Varying Systems and Sampled-Data Systems*, vol. 265 of *Lecture Notes in Control and Information Sciences*, Springer, Berlin, Germany, 2001.

[10] T. Jacobsen and K. West, "Diffusion impedance in planar, cylindrical and spherical symmetry," *Electrochimica Acta*, vol. 40, no. 2, pp. 255–262, 1995.

[11] C. Wang, "Kinetic behavior of metal hydride electrode by means of *ac*-impedance," *Journal of the Electrochemical Society*, vol. 145, no. 6, pp. 1801–1812, 1998.